

## Maya Blue: A Computational and Spectroscopic Study

Roberto Giustetto,<sup>\*,†</sup> Francesc X. Llabrés i Xamena,<sup>‡</sup> Gabriele Ricchiardi,<sup>§</sup> Silvia Bordiga,<sup>§</sup> Alessandro Damin,<sup>§</sup> Roberto Gobetto,<sup>§</sup> and Michele R. Chierotti<sup>§</sup>

Dipartimento di Scienze Mineralogiche e Petrologiche, University of Turin, via V. Caluso 35, 10125 Turin, Italy, C/Joan Rosselló de Son Fortesa, 13, Alaró 07340, Spain, and Dipartimento di Chimica IFM, University of Turin, via Giuria 7, 10125 Turin, Italy

Received: March 31, 2004; In Final Form: May 11, 2005

Maya Blue pigment, used in pre-Colombian America by the ancient Mayas, is a complex between the clay palygorskite and the indigo dye. The pigment can be manufactured by mixing palygorskite and indigo and heating to  $T > 120$  °C. The most quoted hypothesis states that the dye molecules enter the microchannels which permeate the clay structure, thus creating a stable complex. Maya Blue shows a remarkable chemical stability, presumably caused by interactions formed between indigo and clay surfaces. This work aims at studying the nature of these interactions by means of computational and spectroscopic techniques. The encapsulation of indigo inside the clay framework was tested by means of molecular modeling techniques. The calculation of the reaction energies confirmed that the formation of the clay–organic complex can occur only if palygorskite is heated at temperatures well above the water desorption step, when the release of water is entropically favored. H-bonds between the clay framework and the indigo were detected by means of spectroscopic methods. FTIR spectroscopy on outgassed palygorskite and freshly synthesized Maya Blue samples showed that the presence of indigo modifies the spectroscopic features of both structural and zeolitic water, although no clear bands of the dye groups could be observed, presumably due to its very low concentration. The positions and intensities of  $\delta(\text{H}_2\text{O})$  and  $\nu(\text{H}_2\text{O})$  modes showed that part of the structural water molecules interact via a hydrogen bond with the C=O or N–H groups of indigo. Micro-Raman spectra clearly evidenced the presence of indigo both in original and in freshly synthesized Maya Blue. The  $\nu(\text{C}=\text{O})$  symmetric mode of Maya Blue red-shifts with respect to pure indigo, as the result of the formation of H-bonds with the nearest clay structural water. Ab initio quantum methods were applied on the indigo molecule, both isolated and linked through H-bonds with water, to calculate the magnitude of the expected vibrational shifts. Calculated and experimental vibrational shifts appeared to be in good agreement. The presence of a peak at 17.8 ppm and the shift of the N–H signal in the  $^1\text{H}$  MAS NMR spectrum of Maya Blue provide evidence of hydrogen bond interactions between indigo and palygorskite in agreement with IR and ab initio methods.

### Introduction

Maya Blue (MB hereafter) is a blue pigment used in Central America, mostly in Mexico, from VIII to XVI century A.D. to decorate pottery, statues, and wall paintings. Its color shows various hues, ranging from light turquoise to dark greenish blue. MB shows a remarkable stability: it remains unaffected when attacked by acids (HCl and  $\text{HNO}_3$ ), alkali, and any sort of organic solvent. MB was rediscovered in 1931 by Merwin<sup>1</sup> while he was exploring the remains of the Temple of the Warriors in Chichén Itza (Yucatan). Despite the many archaeological discoveries exploited since then, its composition remained a mystery for the next 30 years. Towards the end of 1950s, XRPD proved the presence of MB in the clay palygorskite.<sup>2</sup> The exceptional stability is undoubtedly the most stunning characteristic of MB. Even after centuries, the splendid murals of Bonampak and Chichén Itza maintain their vivid aspect. This fact focused the interest of the scientific community to uncover the secrets of its beauty and durability. Palygorskite  $[(\text{Mg},\text{Al})_4(\text{Si})_8(\text{O},\text{OH},\text{H}_2\text{O})_{26}\cdot n\text{H}_2\text{O}]$  is a fibrous clay, first described in

1860 and found in the mineral basin of Palygorsk,<sup>3</sup> whose structure was illustrated in 1940<sup>4</sup> and later reviewed and refined by several authors.<sup>5–10</sup> Palygorskite is a dioctahedral clay, formed by discontinuous octahedral layers elongated in the *c*-direction alternated with continuous tetrahedral ones. The apexes of the  $\text{SiO}_4$  tetrahedra point alternatively upward and downward every two chains, causing the structure to be crossed by microchannels in the *c*-direction. Palygorskite is a mixture of two polymorphs: monoclinic (space group:  $C2/m$ ) and orthorhombic ( $Pbmn$ ).<sup>6,7</sup> It contains, at room temperature, three different types of adsorbed water molecules, with increasing thermal stability: (i) loosely bound (physisorbed) water, covering the surface of each fiber; (ii) weakly bound water molecules in the channels (zeolitic water); and (iii) tightly bound water molecules completing the coordination of the (Mg,Al) cations at the borders of each octahedral layer (structural water). Besides, palygorskite contains structural hydroxyl groups (Mg–OH and Al–OH). The presence of palygorskite in MB did not explain the pigment color since the clay is colorless. Gettens<sup>2</sup> proposed that the color of MB could be caused by the presence of an organic dye, perhaps indigo. Indigo was well-known to the Mayas, who extracted it from the leaves of *Indigofera suffruticosa*.<sup>11</sup> A pigment analogous to MB (in color and stability) was synthesized by mixing palygorskite and indigo

\* Corresponding author. roberto.giustetto@unito.it.

<sup>†</sup> Dipartimento di Scienze Mineralogiche e Petrologiche, University of Turin.

<sup>‡</sup> C/Joan Rosselló de Son Fortesa.

<sup>§</sup> Dipartimento di Chimica IFM, University of Turin.

and heating to 120–190 °C for several hours.<sup>12,13</sup> The high temperature plays a fundamental role in the pigment manufacture since unheated palygorskite–indigo mixtures do not show the chemical stability of MB. In previous studies, IR spectroscopy seemed to reveal the presence of indigo both in freshly synthesized and in original MB samples.<sup>11,13</sup> It was suggested that the pigment stability might depend on chemical interactions between palygorskite and indigo, although no details were furnished.<sup>13</sup> The presence of indigo in MB and its role as being responsible for the color is unanimously accepted nowadays,<sup>11,14,15</sup> although an alternative hypothesis, concerning the presence of metallic nanoparticles, was also suggested.<sup>16–18</sup> The weight fraction of indigo in MB is rather low, varying in the range of 0.1–2%. According to the most quoted hypothesis, the dye molecules enter the clay channels once the zeolitic water has been (partially or totally) removed by heating the palygorskite–indigo mixture.<sup>10,19,20</sup> It was suggested that the formation of H-bonds between the indigo carbonyl group and the nearest structural water enables them to anchor the dye inside the clay structure, justifying the pigment stability.<sup>10</sup> This work was aimed to investigate the chemical interactions between palygorskite and indigo. To achieve such a goal, the chemical environment of indigo in MB was carefully studied by means of molecular mechanics, *ab initio* calculations, and spectroscopic techniques such as IR, Raman, and solid-state NMR, typically employed to characterize the interactions between organic molecules and inorganic solids. Indeed, the changes in the  $\delta(\text{H}_2\text{O})$  and  $\nu(\text{H}_2\text{O})$  bands and in the proton chemical shift are known to be useful parameters to detect H-bonds involving water molecules.<sup>21,22</sup> It is worth noticing that such studies may have interesting technological applications in the production of stabilized pigments and nanostructured materials.<sup>23</sup> Indeed, MB is a clear example of a composite material in which an organic guest molecule is encapsulated and organized inside an inorganic host material. Therefore, the study of the host–guest interactions (type and strength) in these composite materials and their influence on the final properties of the guest molecules are of general technological interest.

## Experimental Procedures

The samples of palygorskite (*Sac'lum*) came from the mine of Lorenzo Pech, a few kilometers from Ticul, on the road to Chapab (Chapas, Mexico). A few grams were hand-grinded and purified through dispersion into deionized water, so that the thinner suspended fraction could be separated from the heavier particles and dried. A conventional X-ray powder diffraction pattern, collected on an automated Siemens D-5000 diffractometer using graphite monochromatized Cu K $\alpha$  radiation and a zero-background flat sample holder proved that palygorskite was the only detectable phase. A total of 500 mg of purified palygorskite was subsequently mixed with 10 mg (1% weight) of synthetic indigo (Carlo Erba), heated at 190 °C for 12 h and washed in hot, concentrated HNO<sub>3</sub> (to remove the exceeding, noncomplexed indigo), to produce a freshly synthesized MB sample.<sup>13</sup> The XRPD pattern of such a sample proved to be indistinguishable (same reflection positions and intensities) from the one collected on pure palygorskite, proving that no structural change had occurred during the pigment manufacture. Two original MB specimens (a fragment of a mural painting from the archaeological site of Cacaxtla and a powder sample scratched from the eye of a votive statue of the Mayan god *Tlälöc*, Templo Mayor, Mexico) were also analyzed. Molecular modeling techniques were employed to test the encapsulation of indigo inside the clay framework and to analyze their possible

interactions. The energy and forces of the models were calculated using the *cvff\_aug* force field<sup>24,25</sup> of Accelrys Inc. and the program Discover as implemented in the Materials Studio<sup>26</sup> as the computation engine. This force field describes the organic molecules with a complex valence force field and the inorganic portion using Coulomb interactions and Buckingham repulsions, with specific parameters for clays. Electrostatic and van der Waals energies were calculated with the Ewald method. Starting from the modified crystallographic structures, the internal coordinates and cell parameters of the models were optimized to zero-force and minimum energy values; energies and structures were examined and compared as discussed next. It is worth mentioning that the nature of the force field adopted allows the calculation of absolute binding energies of adsorbates (although within the poor accuracy typical of force field methods). Indigo–water interactions were studied using the B3-LYP functional and the 6-31+G(d,p) basis set, as coded in the Gaussian 98 program;<sup>27</sup> vibrational frequencies were calculated for the optimized stationary points. The reported frequencies were multiplied by a scale factor of 0.96, obtained by comparison of the experimental and calculated frequencies of the formaldehyde molecule. To study the dehydration process in palygorskite, thermogravimetric studies (TGA, DTA) were performed on a thermal analyzer TA Instruments TGA-DTA 2960. Clay samples of about 10 mg were heated under N<sub>2</sub> flux of 100 mL/min, from 25 to 1000 °C, with a 10 °C/min rate. The chemical environment of indigo was studied by means of spectroscopic techniques. Infrared (IR) absorption spectra were collected, under controlled atmosphere, on a FTIR Bruker IFS 66 spectrometer, with a resolution of 2 cm<sup>-1</sup>, and 64 scans for each spectrum were collected. All samples, in the form of thin films supported on Si plates, were previously outgassed under vacuum at 200 °C for 1.5 h to eliminate the zeolitic water. Rehydration experiments were performed by simple exposition to environmental moisture. Other IR spectra in air were collected on a Nicolet spectrometer, equipped with an ATR attachment. Raman spectra were collected on a Renishaw micro-Raman system 1000 on powder and massive samples, excited with a He–Cd laser beam operating at 442 nm in the range of 1100–1800 cm<sup>-1</sup>, addressed with an optical microscope. The scattered signal was collected on a CCD detector located at 180° with respect to the incident beam.

<sup>1</sup>H MAS spectra were acquired on a Varian Infinity Plus 500 spectrometer operating at 499.7 MHz for the <sup>1</sup>H. A pulse duration of 4.0  $\mu$ s was used for the 90° values, and 64 transients were collected for each spectrum with a pulse delay of 10 s. Powdered samples were spun at 25–30 kHz at room temperature in a 2.5 mm zirconia rotor. Proton chemical shifts were externally referenced via the resonance of PDMSO (polydimethylsiloxane) at 0.14 ppm relative to TMS.

## Results and Discussion

**Modeling of the Structure of MB with Molecular Mechanics.** The structure of MB was studied with molecular mechanics (MM) calculations with the following aims: (a) to verify the steric constraints to the placement of indigo in the channels of the clay and the resulting superstructure; (b) to evaluate (although approximately) the energetic of indigo adsorption, in competition with water; and (c) to identify any possible local indigo–clay interaction, relevant per se and for the interpretation of the spectroscopic experiences. Starting from the experimental structures of orthorhombic and monoclinic palygorskite<sup>7</sup> (OP and MP hereafter), the occupation of the octahedral layer atoms was fixed to maintain neutrality. The

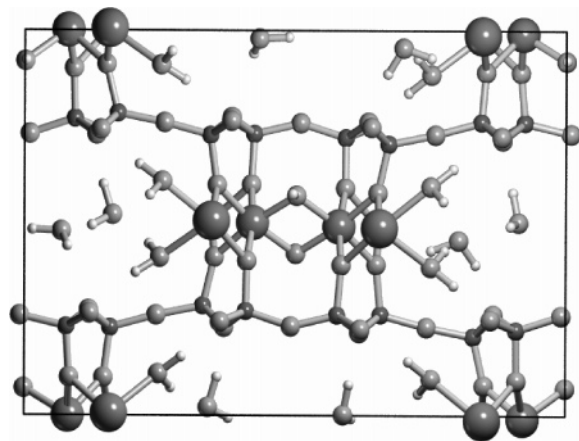


**Figure 1.** Hydrated orthorhombic palygorskite viewed along the *c*-axis. Note the hydrogen bond network formed by zeolitic and structural water molecules.

Mg/Al ratio was 1:1, with Mg atoms occupying all the octahedral positions facing the clay channel (i.e., bound to structural water molecules). This occupation scheme is somehow arbitrary, but preliminary tests showed that the occupation of the octahedral layer has negligible influence on the geometry of the models. Hydrogen atoms were added manually, at sterically acceptable positions, to crystallographic oxygens of structural water, zeolitic water, and hydroxyl groups, obtaining the initial models for hydrated clay (OPW and MPW). If we assume the formation of a palygorskite–indigo complex, its structure requires the dye molecule to have nonrandom positions inside the clay lattice. If so, indigo can affect both the symmetry and the lattice periodicity of the complex. Indigo was inserted inside the clay structure with an eye toward preserving the symmetry operators of both precursors. The molecule was supposed to lie on the (100) plane inside each channel, with its major axis parallel to the *c*-direction and the inversion center on the C=C bond superposed to the one located at 0,1/2,1/2 of the clay lattice. The accommodation of nonsuperimposing indigo molecules in the clay channels is likely to form a three-cell superstructure (*a,b,3c*) in the *Z*-direction. Despite these simplifications, the position of indigo in MB is affected, in nature, by a multiple-grade disorder.<sup>10</sup> The placement of indigo in the clay channels requires the removal of zeolitic water molecules, which cannot be accommodated aside of the dye molecule. The  $1 \times 1 \times 3$  supercells containing two complete indigo molecules were constructed both for MP and OP. The symmetry of both supercells was reduced to P1, to allow the clay structure to relax without constraints under the effect of the adsorbate. All the zeolitic water molecules were removed. These models will be called OPI and MPI hereafter, for orthorhombic and monoclinic polymorph, respectively. A mixed indigo–water occupation may be realistic on the grounds of previous experimental data<sup>10</sup> and could be modeled using larger blocks of structure, but this aspect was not considered.

As far as hydrated palygorskite is concerned (Figure 1), the oxygen atoms of the zeolitic water molecules (eight per unit cell) occupy positions close to those of the starting model. The hydrogen atom positions form a continuous H-bond network among the zeolitic water molecules and with the structural water molecules. Optimized MB models (OPI and MPI) show only minor distortions with respect to the initial symmetric structures (Figure 2). The indigo molecules maintain their positions in the middle of each channel, although their geometry appears slightly distorted as a result of interactions with the neighboring structural water. A direct evidence of this loss of planarity of

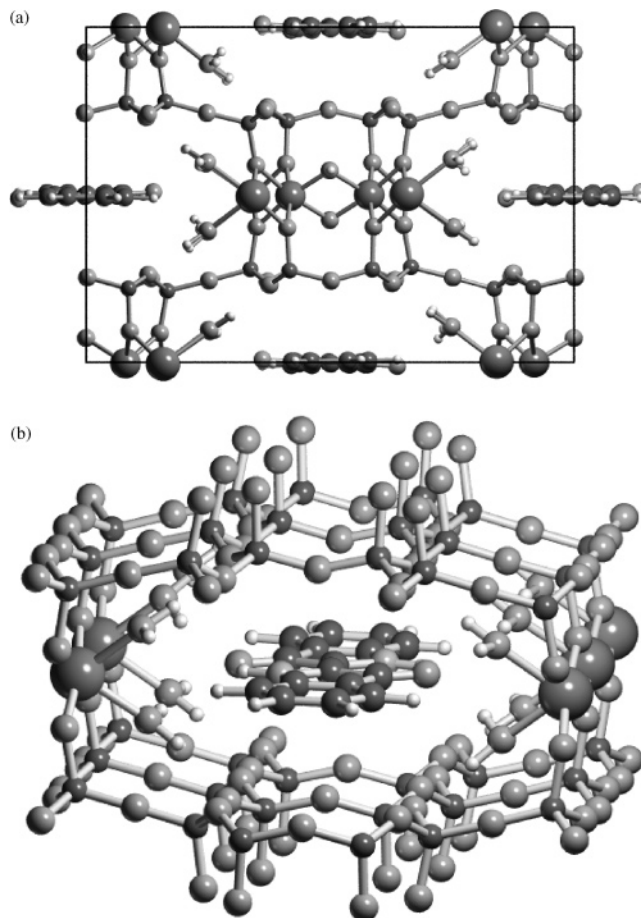
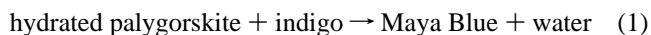


**Figure 2.** Adopted Maya Blue model, consisting of a  $1 \times 1 \times 3$  palygorskite supercell hosting two complete indigo molecules. The figure represents the optimized monoclinic structure projected on the 001 plane (a) and a section of the channel tilted to highlight the position of indigo (b).

the indigo molecule was collected using Raman spectroscopy.<sup>28</sup> H-bonds between the indigo C=O and the structural water molecules firmly anchor the dye molecule to the clay structure, with an average  $\text{H}\cdots\text{O}=\text{C}$  distance of 174 pm for MP and 185 pm for OP. On the contrary, no evident  $\text{N}-\text{H}\cdots\text{O}$  H-bond was detected, due to the unfavorable position of the oxygen atoms of water, strongly coordinated to the octahedral cations. The lattice energy of the orthorhombic polymorphs is always slightly higher than that of the monoclinic ones. The energy differences, which account for the relative stability of the structures, are 3.3, 15.3, and 4.5 kcal/mol per u.c. for dehydrated palygorskite, hydrated palygorskite, and MB, respectively. The average binding energy of zeolitic water molecules is 15.2 kcal/mol (per  $\text{H}_2\text{O}$  molecule) on OPW and 16.8 kcal/mol on MPW, indicating that the monoclinic polymorph is slightly more hydrophilic than the orthorhombic one, as confirmed by other studies.<sup>29</sup> The binding energy of indigo is 43.1 kcal/mol in OPI and 45.0 kcal/mol in MPI: this may indicate that indigo adsorption on MP might be preferred, although previous results seemed to assess an opposite behavior.<sup>10</sup> Although the indigo molecule can be strongly adsorbed into the clay channels, the energy change for the reaction



as calculated from the energies reported previously is always positive. The reaction energy is 279.8 kcal/mol for the orthorhombic polymorph and 313.8 kcal/mol for the monoclinic one.



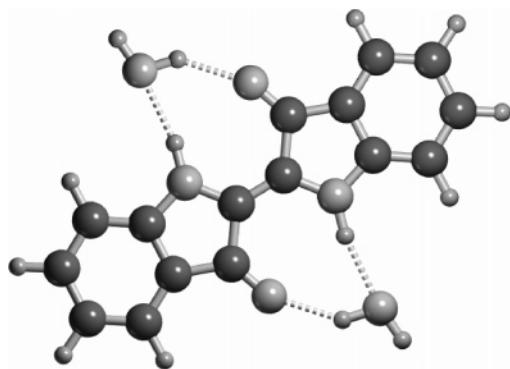


**Figure 3.** Indigo–water complex used to calculate the magnitude of the vibrational shifts caused by the formation of H-bonds.

This difference is mainly due to a higher hydrophilicity of MP, as already stated previously. The high positive value of these reaction energies, together with kinetic considerations, may explain why the stable pigment is formed only after treatment of the impregnated clay at temperatures above the water desorption step, when the release of water is entropically favored. Previously, a paper by Fois et al. describing MB modeling with a similar approach appeared.<sup>30</sup> The main differences among the two adopted procedures are that (a) the work of Fois et al.<sup>30</sup> used molecular dynamics simulations to obtain insight into the sorption dynamics of the indigo–clay complex, adopting a modified version of the cvff\_aug force field, while this one dealt with static minimum energy structures only; (b) the models of MB adopted in the previous work<sup>30</sup> are more diluted since they contain a single indigo molecule in a  $2 \times 2 \times 7$  hydrated supercell; (c) cutoffs (1 nm) for vdW interactions were used by Fois et al.<sup>30</sup> (as well as in other works<sup>10</sup>), while the present study used an exact periodic summation method; and (d) both palygorskite polymorphs were investigated in the current study, while that of Fois et al.<sup>30</sup> was confined to the monoclinic structure. Besides, the results of the two studies are in fairly good agreement and somehow complementary because while the current study deals with a static model with the maximum concentration of adsorbates (allowing the calculation of thermochemical properties such as binding energies), the other one<sup>30</sup> describes a dynamic model with a realistic dual occupation (water and indigo) of the host clay. In both works,  $\text{C}=\text{O} \cdots \text{H}$  bonds are observed between the dye and the clay, but  $\text{N}-\text{H} \cdots \text{O}$  bonds are not. The position of an indigo molecule inside the clay framework is also very similar. As already stated previously,<sup>10</sup> both works agree on the fact that no periodic MB model can be built from the OP coordinates proposed by Artioli and Galli.<sup>9</sup>

**Modeling of the Indigo–Water Hydrogen Bonds with Ab Initio Quantum Methods.** The detection of  $\text{C}=\text{O} \cdots \text{H}$  hydrogen bonds in the structures simulated with molecular mechanics raised the question as to whether this kind of interaction could be detected by spectroscopic methods. The magnetic, electronic, and vibrational transitions of the indigo–clay complex should differ from those of the isolated moieties, as a result of the reciprocal interactions. Attention was focused on the actual extent of the expected shifts since the very low concentration ( $<2\%$ ) of the guest molecule in the host clay<sup>10</sup> might cause only hardly detectable variations. Ab initio calculations concerning the interaction of an indigo molecule with water were performed, to ascertain the magnitude of the vibrational shifts. The structure of the indigo–water complex is shown in Figure 3. The main calculated frequencies and expected shifts are listed in Table 1. The model calculated for the vibrational structure of indigo is affected by evident limits, to be taken into proper consideration when discussing the spectroscopic behavior of MB. In the optimized model, each water molecule forms two hydrogen bonds, one as a H-donor with  $\text{C}=\text{O}$  and the other as a H-acceptor from  $\text{N}-\text{H}$ . The  $\text{C}=\text{O} \cdots \text{H}$  and  $\text{N}-\text{H} \cdots \text{O}$  distances are 191 and 201 pm, respectively. This local structure differs sensibly from the one in which indigo interacts with the structural water molecules of palygorskite (Figure 2). In the MB structure, the oxygen atoms of structural water are farther from the indigo molecule than those of the calculated indigo–water adduct since they are coordinated to the cations of the octahedral layer. The complex described in Figure 3 has therefore to be regarded as a generic probe of the response of the indigo vibrations when involved in H-bond perturbations, without any attempt to interpret this response in terms of given structural features. Nevertheless, these generic indications are extremely precious in analyzing the spectroscopic data collected on MB. The calculated vibrational frequencies for the isolated indigo molecule are in agreement with those measured in previous works.<sup>31</sup> Note that the  $\text{C}=\text{O}$  stretching mode is split into two bands (symmetric and antisymmetric), which undergo different shifts ( $-13$  and  $-3$   $\text{cm}^{-1}$ , respectively) upon interaction with water.

**Thermal Studies.** A thermogravimetric study (TGA, DTA) was performed on the Mexican palygorskite to estimate its exact sorption capacity. In fact, palygorskite samples coming from different sites may have different structural and compositional features, which might affect their affinity to absorb water. In addition, such studies allowed us to estimate accurately the temperature values and times in which the different types of water molecules are desorbed from the structure, to plan a correct thermal treatment for the spectroscopic experiences, which required the sample to be outgassed. At increasing

**TABLE 1: Selected Corrected Vibrational Modes of the Indigo Molecule ( $\text{cm}^{-1}$ ), Isolated and Interacting with Two Water Molecules (see Figure 3)**

vibrational mode	indigo	indigo + 2H <sub>2</sub> O	shift ( $\text{cm}^{-1}$ )
free OH stretch		3760, 3760	
OH stretch (H bonded to O=C)		3563, 3565	
H–O–H bend		1533, 1525	
H–O–H bend coupled with N–H stretch		1578	
N–H stretch	3468, 3469	3432, 3431	−36, −38
C–H stretch	3087–3060	3090–3060	
symmetric C=O stretch, strongly coupled with C=C stretch	1692	1679	−13
antisymmetric C=O stretch	1635	1632	−3
C–C ring modes	1616–1564		
N–H in-plane bend	1460, 1393	1389, 1357	−71, −36
C–N asymmetric stretch	1340		
C–N–C symmetric stretch	1233	1327	+94
N–H in-plane bends coupled with C–H and C–C modes	1193, 1148, 1118, 1047	1219, 1148, 1118, 1036	+26, 0, 0, −11

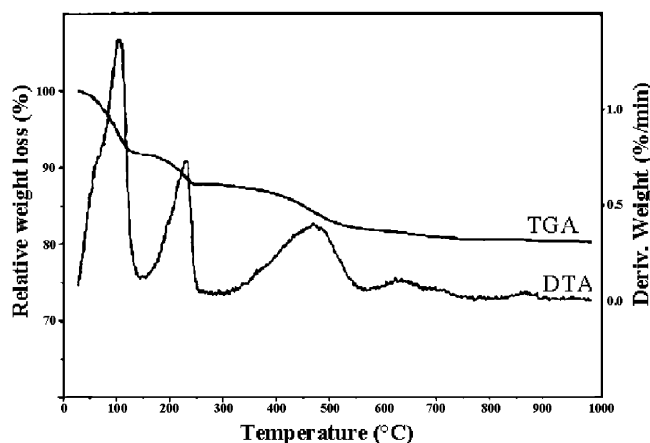


**Figure 4.** Observed TGA and DTA curves of palygorskite. Vertical scale for the TGA curve is weight loss percent.

temperature, dehydration of palygorskite proceeds in four distinct steps (Figure 4), whose exact positions slightly depend from the adopted experimental conditions: (i) the first loss of weight occurs at about 110–120 °C, corresponding to a sharp endothermic peak in the DTA. This is due to the desorption of loosely bound (physisorbed) water and some zeolitic water; (ii) another endothermic peak occurs at 220–230 °C, evidencing the loss of the residual fraction of zeolitic water and perhaps of some of the weakly bound structural water molecules.<sup>8,32,33</sup> The global weight loss for these two steps is about 13%; (iii) at 450–480 °C, another large endothermic peak in the DTA (5% weight loss) can be attributed to the release of structural water, with the formation of palygorskite anhydride;<sup>5</sup> and (iv) a low but progressive weight loss is observed until 700 °C, when dehydroxylation and phase transformation to clino-enstatite occur.<sup>5,34</sup> No weight loss is observed above 700 °C.

**FTIR Spectroscopy.** IR spectra were collected on palygorskite, indigo, and on two MB samples, one artificially synthesized (<1% indigo weight fraction) and one original (Templo Mayor, Mexico). For the sake of brevity, only the spectroscopic features of the freshly synthesized MB pattern are discussed. The results obtained with the ancient pigment are analogous, but the spectra are of a worse quality (presumably deriving from the scarce purity of the sample).

**Palygorskite.** All different types of adsorbed water molecules (physisorbed, zeolitic, and structural) present their own spectroscopic features in the 3800–3000  $\text{cm}^{-1}$  spectral range. The IR spectrum of palygorskite outgassed at 200 °C under dynamic vacuum for 1.5 h (Figure 5) presents main bands (or shoulders) peaking at 3661 (shoulder), 3644 (sharp band), 3609 (shoulder), and broad bands at 3582 and 3525  $\text{cm}^{-1}$ , as well as minor (broad) components at ca. 3380 and 3275  $\text{cm}^{-1}$ . In the  $\delta(\text{H}_2\text{O})$  spectral region, a band is also observed at 1621  $\text{cm}^{-1}$ . Rehydration of the sample brings out clear spectral changes, consisting of: (i) partial erosion of the 3644  $\text{cm}^{-1}$  band, with concomitant formation of a new peak at 3613  $\text{cm}^{-1}$  (note the presence of an isosbestic point at 3637  $\text{cm}^{-1}$ ); (ii) the intensity increase of the band at 3525  $\text{cm}^{-1}$ , whose final envelope becomes complex, with a new component at about 3545  $\text{cm}^{-1}$ ; (iii) the intensity increase of the bands at 3380 and 3275  $\text{cm}^{-1}$  upon rehydration, which become broader; (iv) the band at 1621  $\text{cm}^{-1}$ , basically unaffected by rehydration, shows the formation of a new (complex) IR absorption in its high-frequency side, covering the range from 1640 to 1675  $\text{cm}^{-1}$ . According to the existing literature,<sup>34–36</sup> the bands corresponding to the O–H stretching mode of structural water are those at 3644, 3609, 3582, and 3525  $\text{cm}^{-1}$ , together with the deformation mode at

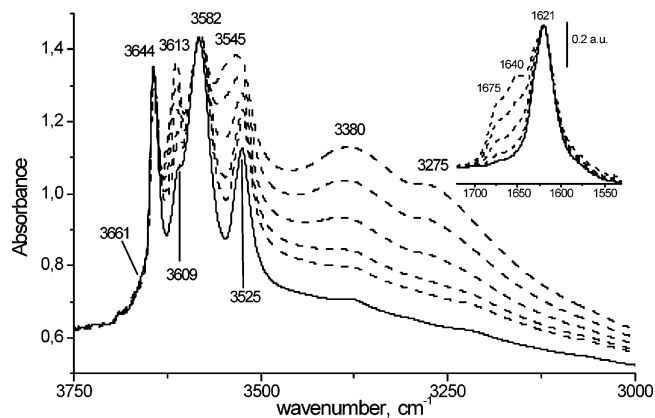


**Figure 5.** IR spectrum of palygorskite outgassed at 200 °C for 1.5 h (continuous line) and progressively rehydrated (dotted lines).

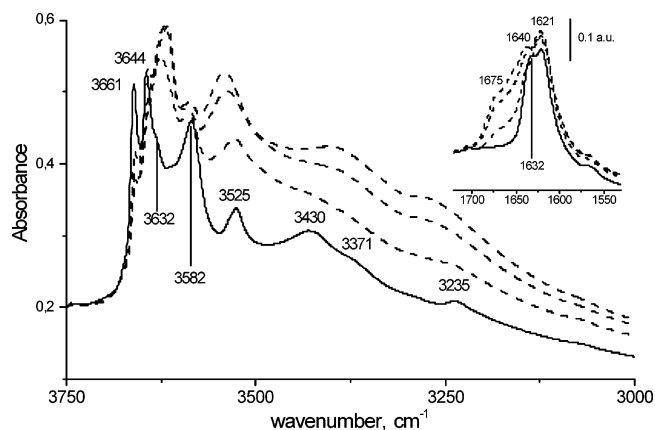


**Figure 6.** IR spectrum of freshly synthesized Maya Blue outgassed at 200 °C for 1.5 h (continuous line) and progressively rehydrated (dotted lines).

1621  $\text{cm}^{-1}$ . Note that these are the most prominent bands appearing in the spectrum of palygorskite outgassed at 200 °C. Outgassing under vacuum at 200 °C causes the desorption of most of the zeolitic water (released above 230 °C in air). However, minor components at 3380 and 3275  $\text{cm}^{-1}$  reveal that a small amount of this type of water is still present. Upon progressive rehydration of the sample (Figure 5), zeolitic water molecules become dominant as indicated by the increased intensity of the related O–H bands (i.e., those at 3380 and 3275  $\text{cm}^{-1}$ ) and by the appearance of the complex absorption at 1640–1675  $\text{cm}^{-1}$ . Zeolitic water interacts with structural water, as indicated by the changes observed in the 3644–3525  $\text{cm}^{-1}$  spectral region.

**Freshly Synthesized MB (Palygorskite + Indigo).** The bands due to water molecules in the IR spectrum of artificial MB, outgassed at 200 °C under dynamic vacuum for 1.5 h (Figure 6), seem to be very similar to those observed for pure palygorskite. However, clear differences are present both in their relative intensities and in their positions. The most important changes can be summarized as follows: (i) the intensity of the band at 3661  $\text{cm}^{-1}$  (practically absent in palygorskite) is dramatically increased; (ii) a new band (shoulder), not detected in pure palygorskite, is observed at 3632  $\text{cm}^{-1}$ ; (iii) the bands corresponding to residual zeolitic water (at 3380 and 3275  $\text{cm}^{-1}$  in palygorskite) are shifted toward higher wavenumbers (i.e., at 3430 and 3371  $\text{cm}^{-1}$ ); (iv) a very weak band, almost undistinguishable in pure palygorskite, is observed at 3235  $\text{cm}^{-1}$ ; and (v) the deformation band at 1621  $\text{cm}^{-1}$  is now accompanied by a new component at 1632  $\text{cm}^{-1}$  (absent in palygorskite). The changes in the IR spectrum upon rehydration are completely

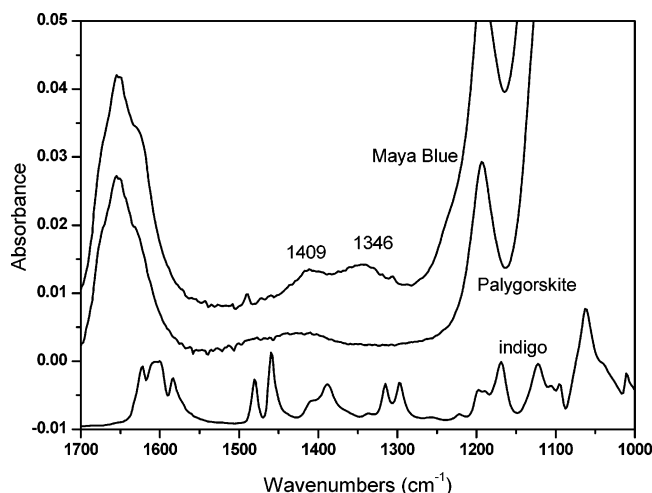


**Figure 7.** ATR-IR spectra of synthetic indigo, palygorskite, and Maya Blue in air. Spectra have been vertically shifted for clarity.

analogous to those previously observed for pure palygorskite. Note that the band at  $1632\text{ cm}^{-1}$  cannot be ascribed to residual zeolitic water in the sample, as it does not grow upon rehydration. Therefore, its origin must be of a different nature. In the region of  $1000\text{--}1600\text{ cm}^{-1}$  (not reported), these spectra differ from those of pure palygorskite for the presence of a weak band at  $1565\text{ cm}^{-1}$ , which will be discussed later. Since Leona et al.,<sup>37</sup> using FTIR microspectroscopy on both original and freshly synthesized MB samples compressed in a diamond anvil, observed in this region some vibrational features of the dye molecule, an attempt was made to investigate the very same spectral region with higher sensitivity, using an attenuated total reflectance (ATR) technique. The ATR spectra of crystalline indigo, palygorskite, and freshly synthesized MB are reported in Figure 7. The following considerations can be made: (i) the spectrum of crystalline indigo is in excellent agreement with that published in previous literature;<sup>31</sup> (ii) the comparison between the spectrum of palygorskite and the spectrum of MB shows only very minor differences, the latter showing additional weak and broad bands ( $1409$  and  $1346\text{ cm}^{-1}$ ) absent in the clay pattern. Note that no evident correlation can be observed between such bands and those corresponding to the characteristic frequencies of the solid dye; (iii) the band at  $1632\text{ cm}^{-1}$ , present in the outgassed MB spectrum, cannot be observed in the ATR pattern due to the fact that the sample, being at air, is partially hydrated. A plausible origin of the bands observed at  $1565$  (outgassed MB: Figure 6),  $1409$ , and  $1346$  (ATR, MB at air: Figure 7)  $\text{cm}^{-1}$  is the presence of isolated, perturbed indigo molecules in the pigment, whose vibrations occur at different frequencies with respect to those observable for the crystalline dye. The discrepancy between the discussed spectra and those published by Leona et al.<sup>37</sup> may be further explained by the higher indigo content of their synthesized MB samples (selected particles from an averaged 2 wt % indigo).

The presence of indigo, although not directly detected, modifies the spectroscopic features of both structural and zeolitic water since the IR absorption patterns of palygorskite and freshly synthesized MB differ from one another (Figures 5 and 6). This fact indicates that the chemical environment inside the clay channels clearly changes as a consequence of the indigo encapsulation. In general, a less polar medium inside the clay channels is found in MB rather than in pure palygorskite: note, for instance, the higher frequencies of the bands of zeolitic water ( $3430$  and  $3371\text{ cm}^{-1}$  for MB and  $3380$  and  $3275\text{ cm}^{-1}$  for palygorskite). The assignment of the band located at  $1632$  merits

further discussion. The spectrum of pure indigo (ATR: Figure 7) shows a band at  $1623\text{ cm}^{-1}$ , which corresponds to the  $\nu$ -( $\text{C}=\text{O}$ ) antisymmetric stretching mode of the carbonyl groups (calculated frequency:  $1635\text{ cm}^{-1}$ ; Table 1). Thus, one may be tempted to assign the band at  $1632\text{ cm}^{-1}$  in the MB spectrum to the antisymmetric  $\text{C}=\text{O}$  stretching mode of indigo, slightly perturbed, due to interactions with water molecules in the clay. This assignment finds objection in the following considerations: (i) the intensity of this band is too high, considering the very low indigo content of the MB sample ( $<1\%$ ); (ii) other intense bands characteristic of the indigo molecule (such as the  $\text{C}-\text{C}$  stretching ring modes at  $1480$  and  $1459\text{ cm}^{-1}$ ; Figure 7) are completely absent in the spectrum of MB; and (iii) the calculated frequency shift of this stretching mode when engaged in a H-bond with a water molecule is only  $3\text{ cm}^{-1}$  (see Table 1). On this basis, an alternative assignment is needed. The band at  $1632\text{ cm}^{-1}$  may be tentatively ascribed to the  $\delta(\text{H}_2\text{O})$  mode of a particular kind of structural water molecule, in a slightly different chemical environment with respect to those responsible for the main band at  $1621\text{ cm}^{-1}$ . As this type of water molecules is absent in pure palygorskite, they must be related to the presence of indigo. Structural water molecules interacting (via H-bond) with the  $\text{C}=\text{O}$  (or  $\text{N}-\text{H}$ ) groups of indigo seem the most likely origin for the band at  $1632\text{ cm}^{-1}$ , although reciprocal interactions among structural water molecules cannot be excluded. The same structural water/indigo interactions may also explain the changes observed in the  $3700\text{--}3300\text{ cm}^{-1}$  region. For instance, the band at  $3661\text{ cm}^{-1}$  in the MB spectrum is dramatically increased with respect to pure palygorskite. The assignment of this band is uncertain. Both the high frequency of this  $\text{O}-\text{H}$  stretching mode and its sharp shape may suggest the assignment to structural water molecules vibrating against the nonpolar part of indigo, located inside the clay channels. Besides, its disappearance upon hydration implies that such OH groups must be accessible to water even in the presence of indigo, a fact hardly explainable considering the tight fitting of the dye in the pores, as indicated by simulations, but plausible on the clay surface. An alternative explanation is the attribution of this high-frequency component to a collective vibration of water molecules on two different cationic sites (e.g., Mg and Al in octahedral coordination). In fact, in clays, the vibrations of  $\text{H}_2\text{O}$  molecules in different sites are known to combine according to the crystal symmetry, to give complex groups of bands.<sup>35</sup> The presence of indigo may change the degree of coupling of the water modes, either by direct interactions or by changing the local symmetry, increasing their intensity. The disappearance with hydration may be due to the formation of hydrogen bonds, shifting all modes to lower frequencies.

**Raman Spectroscopy.** Raman spectra were collected on synthetic indigo (Carlo Erba) and on two MB samples, one freshly synthesized ( $<1\text{ wt \%}$  indigo) and one original (Cacaxtla, Mexico). Data collected on pure palygorskite showed no appreciable vibrational signals, due to the extremely high fluorescence, as already reported in the literature.<sup>28,37</sup> The comparison between our Raman spectra and those of recent works<sup>28,37</sup> is, however, complicated due to resonance effects: in fact, in having the indigo molecule absorption bands both in the visible and in the UV regions, the intensity of the Raman signals is very sensitive to the excitation wavelength (our spectra:  $325\text{ nm}$ ; previous works:  $785^{37}$  and  $514.5\text{ nm}^{28}$ ).

**Indigo.** The spectrum collected on pure crystalline indigo excited with a  $325\text{ nm}$  laser is shown in Figure 8a; note that the lower frequency region was obtained with a slower scan to achieve a better sensitivity. The positions of the vibrational



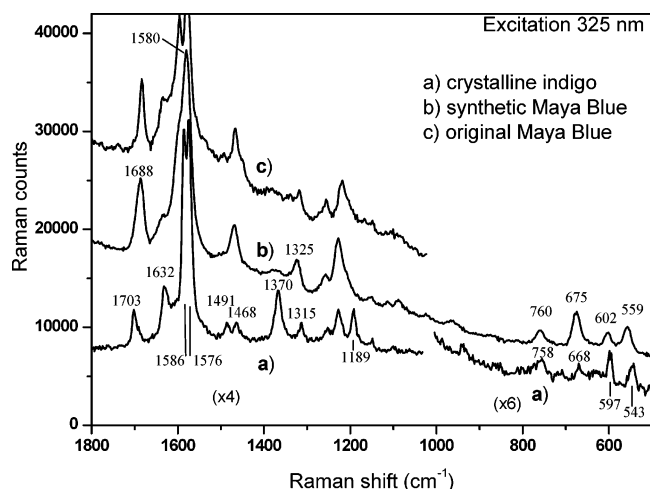


**Figure 8.** Raman spectra of crystalline indigo (a) and freshly synthesized (b) and original Maya Blue (c), scaled and shifted for clarity.

Raman features are comparable to those obtained in recent works,<sup>28,37</sup> although significant differences occur in the observed intensities, due to the different excitation lines employed. Such discrepancies can be summarized as follows: (i) a weak peak reported by Witke et al.<sup>28</sup> at approximately 1540  $\text{cm}^{-1}$  cannot be observed in our spectra, nor in the one collected by Leona et al.;<sup>37</sup> (ii) very strong signals can be observed in our spectra at 1370  $\text{cm}^{-1}$  (attributed to the in-plane bending of the N–H, coupled with C–H, groups) and 1189  $\text{cm}^{-1}$  (assigned to a  $\nu(\text{C}=\text{C})$  in rings, strongly enhanced by resonance): the former is observed also by Witke et al.,<sup>28</sup> while in Leona et al.<sup>37</sup> it is substituted by a weak band at 1365  $\text{cm}^{-1}$ ; the latter is absent in both works; (iii) in the low-frequency region (500–1100  $\text{cm}^{-1}$ ), weaker signals can be observed both in our spectra and in Witke et al.,<sup>28</sup> while strong bands appear in the profile of Leona et al.;<sup>37</sup> this might be explained with resonance enhancement of the bands associated with C–H and N–H vibrations, whose harmonics and combination bands lie in the vicinity of the excitation line used by Leona et al.;<sup>37</sup> and (iv) the band at 635  $\text{cm}^{-1}$  cited by Leona et al.<sup>37</sup> is almost undistinguishable in our spectra. A thorough assignment of the vibrational spectra of indigo was given by Tatsch et al.<sup>31</sup> and substantially confirmed by our calculations (see Table 1).

The band at 1703  $\text{cm}^{-1}$  is assigned to the symmetric stretching mode of the two C=O groups (calculated frequency: 1692  $\text{cm}^{-1}$ ; Table 1), strongly coupled with the C=C stretch. The antisymmetric stretching C=O mode (calculated frequency: 1635  $\text{cm}^{-1}$ ) is not Raman-active; therefore, the band observed in our spectrum at 1632  $\text{cm}^{-1}$  can probably be attributed to collective C–C stretching modes. These modes are also probably responsible for the two most intense bands, occurring at about 1586–1576  $\text{cm}^{-1}$ . Two small peaks appear at 1491 and 1468  $\text{cm}^{-1}$  and can be assigned to C–C stretching modes coupled with C–H deformations.

**Maya Blue.** Since Raman spectroscopy does not detect the vibrational modes of the water molecules, the most impressive aspect of the spectra collected on MB is that the presence of indigo is clearly recognizable. Both in freshly synthesized (Figure 8b) and in original MB (Figure 8c), almost all bands related to the active vibrational modes of indigo are present; moreover, the two patterns are almost identical. The general features observed in the Raman spectra of MB are comparable with those observed in previous works,<sup>28,37</sup> although remarkable differences can be pointed out with regards to the intensities,

as already described for pure indigo. Furthermore, fundamental considerations can be formulated by direct comparison of indigo and freshly synthesized MB Raman spectra: (i) in MB, the two most intense bands of indigo (1576 and 1586  $\text{cm}^{-1}$ ) tend to coalesce in a single peak, centered at 1580  $\text{cm}^{-1}$ ; (ii) a noteworthy difference is the disappearance of a band at 1370  $\text{cm}^{-1}$  present in indigo but absent in the MB spectrum; such vibrational modes, related to  $\delta(\text{N}=\text{H})$  and  $\delta(\text{C}=\text{H})$  modes,<sup>31</sup> implies that the N–H group of indigo is perturbed while encapsulated in the clay, possibly as the result of H-bonds formed with the palygorskite framework. Such variations can be observed in previous works too, although slightly red-shifted (1365  $\text{cm}^{-1}$ ),<sup>37</sup> but here it is exalted by the resonance affecting this band in indigo; (iii) the band at 1315  $\text{cm}^{-1}$  in indigo, attributed to  $\nu(\text{C}=\text{C})$ , shifts to 1325  $\text{cm}^{-1}$  in MB, both in our spectra and in previous works;<sup>28,37</sup> (iv) our MB spectrum shows the disappearance of the  $\nu(\text{C}=\text{C})$  band at 1189  $\text{cm}^{-1}$ , quite intense in indigo: such variations may be explained with a loss of resonance due to a reduced symmetry; (v) at low frequencies, a group of bands located at 543, 597, 668, and 758  $\text{cm}^{-1}$  is slightly shifted toward higher wavenumbers (559, 602, 675, and 760  $\text{cm}^{-1}$ , respectively) passing from indigo to MB, presumably as the result of minor deformations affecting the dye molecule; (vi) the C=O symmetric stretching mode red-shifts from 1703  $\text{cm}^{-1}$  (indigo) to 1688  $\text{cm}^{-1}$  (MB). This change, observable also in Leona et al.,<sup>37</sup> can be interpreted as the result of a perturbation affecting the C=O groups, presumably induced by the formation of a H-bond with the nearest clay structural water. Such a hypothesis is supported by the fact that the calculated shift for the C=O symmetric stretch mode perturbed by a H-bond (–13  $\text{cm}^{-1}$ ; Table 1) is quite similar to the one experimentally observed (–15  $\text{cm}^{-1}$ ); and (vii) another difference implies the band at 1491  $\text{cm}^{-1}$  of indigo spectrum, attributed to  $\nu(\text{C}=\text{C})$ : both in our spectra and in Leona et al.,<sup>37</sup> such a band is present in indigo but disappears in MB, while in Witke et al.,<sup>28</sup> it shows opposite behavior.

Sometimes, the discrepancies between the Raman spectra presented in this work and those appearing in the literature may be even more pronounced. For example, three remarkable bands (1017, 1128, and 1380  $\text{cm}^{-1}$ ) described by Witke et al.<sup>28</sup> in the spectrum of MB and disappearing in indigo, attributed to vibrational modes of the  $B_u$  type in the IR spectrum of the dye molecule, are not visible in our spectra nor in that of Leona et al.<sup>37</sup> In addition, neither we nor Leona et al.<sup>37</sup> do observe any appreciable increase in the intensities of the bands at 1253, 1593, and 1633  $\text{cm}^{-1}$ , described by Witke et al.<sup>28</sup> as the result of the activation of Raman-inactive vibration modes of the  $B_u$  type in indigo.

**Solid-State NMR Spectroscopy.** It is well-known that  $^1\text{H}$  NMR techniques are very useful for detecting and characterizing H-bond interactions.<sup>22</sup> Indeed, the presence of a H-bond leads to a downfield shift of the proton signal of about 2–10 ppm depending on the interaction strength. The polarization of the X–H bond plays a crucial role in determining the proton chemical shift of hydrogen atoms involved in H-bonding (i.e., the stronger the H-bond interaction, the higher the chemical shift value).<sup>38,39</sup> With the development of new NMR instruments, it is now possible to obtain high-resolution  $^1\text{H}$  MAS spectra also in the solid state by spinning the sample at the magic angle at speed higher than 30 kHz. This allows us to overcome the problem of the homonuclear dipolar interaction that in the solid state could be of the order of some tens of kHz. In the past few years, an increasing number of  $^1\text{H}$  MAS studies<sup>40–42</sup> focusing

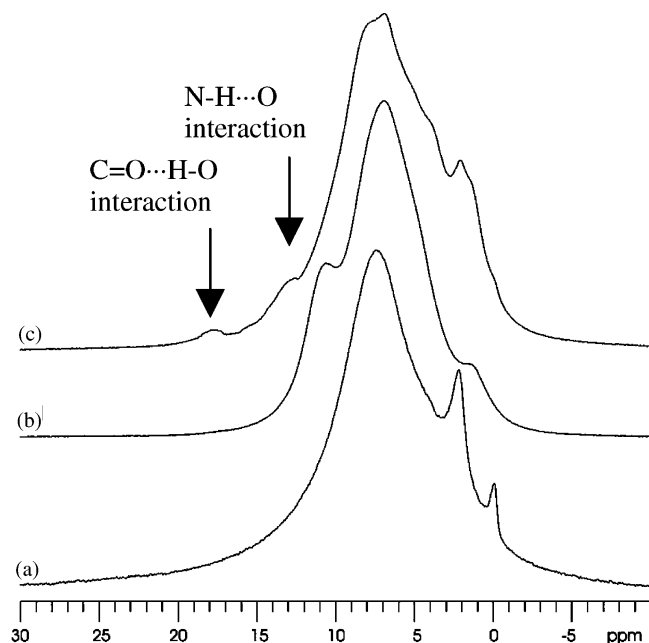


**Figure 9.** High-speed  $^1\text{H}$  MAS NMR spectra of palygorskite (a), indigo (b), and freshly synthesized Maya Blue (c), recorded at 499.7 MHz.

on the full detection of H-bond interactions present in solid-state samples was reported in the literature. It was demonstrated, for instance, that the proton signal for strong H-bonds is shifted to 16–22 ppm for  $\text{N-H}\cdots\text{O}$  interactions and to about 16 ppm for  $\text{F}\cdots\text{H}\cdots\text{F}$  interactions,<sup>43</sup> whereas weak  $\text{N-H}\cdots\text{O}$  and  $\text{O-H}\cdots\text{O}$  interactions are characterized by resonances at values lower than 15–16 ppm.<sup>44</sup>

The  $^1\text{H}$  MAS spectrum of palygorskite (Figure 9a) is dominated by the signals arising from the consistent amount of water in the sample. The main peaks centered at 7.5 ppm and the shoulders at 2.2 and 0.0 ppm are attributed to zeolitic and structural water, to the weakly acid hydroxyl groups, and to silicon impurities, respectively. Nevertheless, it is worth noting that no signal is present in the typical H-bond region (10–20 ppm).

The  $^1\text{H}$  MAS spectrum of indigo (Figure 9b) shows two main resonances at 10.7 and at 7.0 ppm attributed to N–H and to the aromatic protons, respectively.

Identical  $^1\text{H}$  MAS spectra have been observed for the freshly synthesized (Figure 9c) and original MB samples. The spectrum shows a main signal centered at 7.1 ppm, with shoulders at 2.2, 4.4, 7.9, and 13.0 ppm, respectively, and a broad hump at 17.8 ppm. Obviously, the most important feature of this spectrum is the presence of the two resonances in the H-bond region (the peak at 17.8 ppm and the shoulder at 13.0 ppm) since the other signals are reminiscent of the shape of palygorskite resonances. The broad peak at 17.8 ppm (not present either in the clay or in the dye spectra) clearly suggests the presence of a strong H-bond acting between the indigo carbonyl group and the palygorskite structural water (i.e., the  $\text{C=O}\cdots\text{H-O}$  interaction). The formation of a strong interaction is in agreement both with the IR and with the Raman data, indirectly confirming the observed pigment stability. The shoulder at 13.0 ppm is probably due to the interaction between the dye N–H group and an oxygen atom of the clay structural water. The relatively small shift observed for the N–H group, from 10.7 ppm (indigo) to 13.0 ppm (MB), is evidence of the formation of a very weak H-bond in agreement with the Raman data.

## Conclusions

A crystal–chemical study of MB pigment was performed with molecular mechanics and spectroscopic techniques. Such experiences confirmed that the pigment is a complex formed between a clay (palygorskite) and an organic dye (indigo). Modeling studies suggest that the indigo molecules can enter the channels that permeate the palygorskite structure once the zeolitic water is removed through heating. Indigo dimensions are such that it can fit well inside the clay channels. The remarkable stability of the pigment seems to be caused by a specific chemical interaction formed between palygorskite and indigo, namely H-bonds formed between structural water molecules and N–H and C=O groups of the dye. Computational studies suggest the occurrence of H-bonds donated by structural water molecules to the C=O groups of indigo. This interaction is confirmed by the blue-shift of the IR bending mode of structural  $\text{H}_2\text{O}$ , by the red-shift of the Raman C=O stretching mode and by the appearance of the NMR signal of perturbed water. The same techniques also show that such interactions involve only a fraction of the C=O groups and  $\text{H}_2\text{O}$  molecules.

The H-bond interactions of the N–H groups of indigo are clearly evidenced by the shifts of the corresponding Raman bands and by  $^1\text{H}$  NMR experiences. It is remarkable that IR and Raman spectroscopies proved to be complementary techniques, by evidencing the roles of both the donor and the acceptor in H-bonds.

**Acknowledgment.** The authors thank Giacomo Chiari and Constantino Reyes-Valerio for their precious work in the field. Special thanks to Massimo Lazzari for his help in the thermogravimetric analysis. Finally, we are indebted to Prof. Robin K. Harris for providing the possibility of performing the  $^1\text{H}$  MAS NMR spectra at the University of Durham.

## References and Notes

- (1) Merwin, H. E.; Morris, E. H.; Charlot, J.; Morris, A. A. *The Temple of the Warriors at Chichen Itza, Yucatan*; Carnegie Institution of Washington: Washington, DC, 1931; Publication 406.
- (2) Gettens, R. J. *Am. Antiq.* **1962**, 27, 557–564.
- (3) Kukovsky, Y. G.; Ostrovskaya, A. B. *Proc. All Union Mineral. Soc.* **1961**, 90, 598–601.
- (4) Bradley, W. F. *Am. Mineral.* **1940**, 25, 405–410.
- (5) Preisinger, A. *Clays Clay Miner.* **1963**, 10, 365–371.
- (6) Chisholm, J. E. *Can. Mineral.* **1990**, 28, 329–339.
- (7) Chisholm, J. E. *Can. Mineral.* **1992**, 30, 61–73.
- (8) Artioli, G.; Galli, E.; Burattini, E.; Cappuccio, G.; Simeoni, S. N. *Jb. Miner. Mh.* **1994**, 5, 217–229.
- (9) Artioli, G.; Galli, E. *Mater. Sci. Forum* **1994**, 166, 647–652.
- (10) Chiari, G.; Giustetto, R.; Ricchiardi, G. *Eur. J. Mineral.* **2003**, 15, 21–33.
- (11) Reyes-Valerio, C. *Siglo XXI Ed.* **1993**.
- (12) Van Olphen, H. *Science* **1966**, 154, 645–646.
- (13) Kleber, R.; Masschelein-Kleiner, L.; Thissen, J. *Stud. Cons.* **1967**, 12, 41–55.
- (14) Shepard, A. O.; Pollock, H. E. D. *Notes from a Ceramic Laboratory*, Vol. 4; Carnegie Institution of Washington: Washington, DC, 1971; pp 1–32.
- (15) Torres, L. *Mater. Res. Soc. Symp. Proc.* **1988**, 123, 123–128.
- (16) Yacamán, Y. M.; Serra Puche, C. M. *Mater. Res. Soc. Symp. Proc.* **1995**, 352, 3–11.
- (17) Yacamán, Y. M.; Rendón, L.; Arenas, J.; Serra Puche, C. M. *Science* **1996**, 273, 223–225.
- (18) Polette, L. A.; Meitzner, G.; Yacaman, M. J.; Chianelli, R. R. *Microchem. J.* **2002**, 71, 167–174.
- (19) Polette, L. A.; Ugarte, N.; Chianelli, R. R.; Yacamán, J. M. *Discov. Archaeol.* **2000**.
- (20) Polette, L.; Ugarte, N.; Chianelli, R. *Workshop on synchrotron radiation in art and archaeology*; 2000; SSRL.
- (21) Nakanaga, T.; Buchhold, K.; Ito, F. *Chem. Phys.* **2003**, 288, 69–76.
- (22) Garcia-Viloca, M.; Gelabert, R.; Gonzalez Lafont, A.; Moreno, M.; Lluch, J. M. *J. Phys. Chem. A* **1997**, 101, 8727–8733.



- (23) Kuang, W.; Facey, G. A.; Dellier, C.; Casal, B.; Serratos, J. M.; Ruiz-Hitzky, E. *Chem. Mater.* **2003**, *15*, 4956–4967.
- (24) Hill, J. R.; Freeman, C. M.; Subramanian, L. *Use of Force Fields in Materials Modeling*; Wiley-VCH: New York, 2000; pp 141–216.
- (25) Vessal B. *Catalysis and Sorption Consortium Meeting Minutes*; Biosym Technologies Inc.: 1994.
- (26) *Materials Studio 2.2 Discover Module*; Accelrys Incorporated: San Diego, 2002.
- (27) Frisch, M. J.; Trucks, G. W.; Schlegel, H. B.; Scuseria, G. E.; Robb, M. A.; Cheeseman, J. R.; Zakrzewski, V. G.; Montgomery, J. A., Jr.; Stratmann, R. E.; Burant, J. C.; Dapprich, S.; Millam, J. M.; Daniels, A. D.; Kudin, K. N.; Strain, M. C.; Farkas, O.; Tomasi, J.; Barone, V.; Cossi, M.; Cammi, R.; Mennucci, B.; Pomelli, C.; Adamo, C.; Clifford, S.; Ochterski, J.; Petersson, G. A.; Ayala, P. Y.; Cui, Q.; Morokuma, K.; Salvador, P.; Dannenberg, J. J.; Malick, D. K.; Rabuck, A. D.; Raghavachari, K.; Foresman, J. B.; Cioslowski, J.; Ortiz, J. V.; Baboul, A. G.; Stefanov, B. B.; Liu, G.; Liashenko, A.; Piskorz, P.; Komaromi, I.; Gomperts, R.; Martin, R. L.; Fox, D. J.; Keith, T.; Al-Laham, M. A.; Peng, C. Y.; Nanayakkara, A.; Challacombe, M.; Gill, P. M. W.; Johnson, B.; Chen, W.; Wong, M. W.; Andres, J. L.; Gonzalez, C.; Head-Gordon, M.; Replogle, E. S.; Pople, J. A. *Gaussian 98*, Revision A.11; Gaussian, Inc.: Pittsburgh, PA, 2001.
- (28) Witke, K.; Brzezinka, K. W.; Lamprecht, I. *J. Mol. Struct.* **2003**, *661–662*, 235–238.
- (29) Giustetto, R.; Chiari, G. *Eur. J. Mineral.* **2004**, *16*, 521–532.
- (30) Fois, E.; Gamba, A.; Tilocca, A. *Microporous Mesoporous Mater.* **2003**, *57*, 263–272.
- (31) Tatsch, E.; Schrader, B. *J. Raman Spectrosc.* **1995**, *26*, 467.
- (32) Martin Vivaldi, J. L.; Fenoll Hach-Ali, P. In *Differential thermal analysis*; Mackenzie, R. M., Ed.; Academic Press: London, 1970; pp 553–573.
- (33) Jones, B. F.; Galan, E. In *Reviews in Mineralogy*; Bailey, S. W., Ed.; Mineralogical Society of America: Washington, DC, 1988; Vol. 19, pp 631–674.
- (34) Hayashi, H.; Otsuka, R.; Imai, N. *Am. Mineral.* **1969**, *54*, 1613–1624.
- (35) Farmer, V. C., Ed. *Mineralogy Society*; London, 1974.
- (36) Cannings, F. R. *J. Phys. Chem.* **1968**, *72*, 1072–1074.
- (37) Leona, M.; Casadio, F.; Bacci, M.; Picollo M. *J. Am. Inst. Conserv.* **2004**, *43*, 37–52.
- (38) Sternberg, U.; Brunner, E. *J. Magn. Reson., Ser. A* **1994**, *108*, 142.
- (39) Frey, P. A. *Magn. Reson. Chem.* **2001**, *39*, S190–S198.
- (40) Brus, J.; Dybal, J. *Macromolecules* **2002**, *35*, 10038–10047.
- (41) Brus, J.; Dybal, J.; Sysel, P.; Hobzova, R. *Macromolecules* **2002**, *35*, 1253–1261.
- (42) Lorente, P.; Shenderovich, I. G.; Golubev, N. S.; Denisov, G. S.; Buntkowsky, G.; Limbach, H. H. *Magn. Reson. Chem.* **2001**, *39*, S18–S29.
- (43) Hibbert, F.; Emsley, J. *Adv. Phys. Org. Chem.* **1990**, *26*, 255–391.
- (44) McDermott, A.; Ridenour, C. F. In *Encyclopedia of NMR*; Harris, R. K., Ed. Wiley: Chichester, 1996; p 3820.